Nano Energy 97 (2022) 107227

Contents lists available at ScienceDirect

Nano Energy

journal homepage: www.elsevier.com/locate/nanoen

Small-scale, storable paper biobatteries activated via human bodily fluids

Mya Landers [a], Seokheun Choi [a,b,*]

[a] Bioelectronics & Microsystems Laboratory, Department of Electrical & Computer Engineering, State University of New York at Binghamton, Binghamton, NY 13902, USA

[b] Center for Research in Advanced Sensing Technologies & Environmental Sustainability (CREATES), State University of New York at Binghamton, Binghamton, NY 13902, USA

ARTICLE INFO

Keywords:
Microbial fuel cell
Biobattery
Bodily fluid activation
Endospore germination

ABSTRACT

Herein, a fully paper-based biobattery composed of four microbial fuel cell (MFC) units is evaluated, one that can be prepared in advance, stored, and quickly activated with virtually any available fluid. The biobattery uniquely utilizes *Bacillus subtilis* endospores as the storable anodic biocatalyst; the dormant, robust nature of *B. subtilis* endospores should allow for device preinoculation with spores followed by prolonged storage of the fully fabricated paper battery until needed. A germinant paper layer strategically fabricated above the spore-loaded anode layer contains all of the necessary chemical germinants and nutrient components required for the endospores to begin germination, exit dormancy, and return to fully metabolic vegetative bacterial cells that can generate electrical energy. This mechanism allows for the battery to be simply initiated via a wide range of available liquids. Bioelectricity generation of the battery is successfully demonstrated after introduction of a variety of artificial bodily fluids, including saliva, sweat, and urine, along with tap water. Since the biobattery has the capability of serially linking all 4 of its MFCs through simple dynamic folding, the device's total power output can be greatly enhanced; a single biobattery is able to achieve 0.56 V and 2.4 μW, which is beyond the ratings required for their intended application in single-use, disposable sensors. Therefore, this concept of integrating 4 spore-based MFCs into a single biobattery device with a built-in germinant layer offers a potential solution for stable, long-term storable power sources, displaying feasibility for integration with low power, disposable sensor applications.

1. Introduction

With the impending threat of climate change becoming ever clearer, the world has more and more shifted its focus to exploring sustainable, environmentally friendly counterparts to replace existing technologies. One such development is in the field of short-term use, disposable analytic and sensing devices. Cellulose paper-based sensors combat the issue of harmful waste accumulation, as they provide a cheap, biodegradable platform for these analytical applications [1]. Such disposable paper sensors have potential to be used in a wide variety of practical applications; they have most notably made waves in the fields of point-of-care (POC) diagnostics, wearable biosensors for biomonitoring, food and water quality testing, and environmental monitoring [1,2]. The inherent low cost and extensive practicability of paper-based sensors has made them a promising technology both for low-income communities and for remote regions to obtain access to essential services that have traditionally required expensive lab equipment, time-consuming sample preparation, and intensive analytical procedures. However, it is often the case that the existing devices associated with these disposable sensing applications demand the availability of an on-board energy source. Although colorimetric detection methods exist to semi-quantitatively analyse a sample without external energy [3], more precise and reliable evaluation systems require electronics and power sources for signal transduction, amplification, transmission and/or read-out. For example, practical POC-related sensors often require the use of integrated electronics or printed circuit boards (PCBs) to ensure stand-alone devices that can assess a bio-analyte and wirelessly transmit the results to a user [2,4]. Sufficiently powering these systems while preserving their condensed, portable, and low-cost nature calls for a paper-integrable, low-power, safely disposable battery; conventional batteries, such as alkaline or lithium-ion batteries, fail to meet any of these requirements as they are too bulky, overcompensate with

* Corresponding author at: Bioelectronics & Microsystems Laboratory, Department of Electrical & Computer Engineering, State University of New York at Binghamton, Binghamton, NY 13902, USA.

E-mail address: sechoi@binghamton.edu (S. Choi).

https://doi.org/10.1016/j.nanoen.2022.107227
Received 24 January 2022; Received in revised form 24 March 2022; Accepted 30 March 2022
Available online 1 April 2022
2211-2855/

excessive power capabilities, and often result in toxic waste or contain materials of poor disposability [5].

In recent years, an alternative power solution has been extensively investigated, promising to address all of the concerns currently restricting disposable paper sensors: paper-based microbial fuels cells (MFCs) [6–10]. MFCs harvest electrical energy from organic materials using bacterial catalysts [7]. Electrons are generated as a by-product of the bacterial respiratory cycle, and some specific types of bacteria—termed "exoelectrogens" or simply "electrogens"—are capable of exporting these electrons to their external environment and donating them to a naturally-occurring electron acceptor molecule or, in the case of MFCs, even an intentionally-placed electrode [11]. In this way, sustainable electrical energy can be produced in a safe, low-cost manner, providing power on the micro- or milli-watt scale [7,8]. Furthermore, the capability of fabricating these types of fuel cells on paper substrates enables the development of cheap, one-use, low power biobatteries, which are ideal for integration within disposable sensor platforms. However, operation of these paper biobatteries requires 3 main components: (1) the paper battery architecture consisting of the anode/cathode electrodes and an ion exchange membrane, (2) the live exoelectrogens to act as the biocatalysts, and (3) the nutrient-rich liquid media, or "anolyte," which supplies the life-sustaining nutrients for the bacteria [6]. In research settings, supplying the bacteria and anolyte components entail sample preparation and culturing processes, requiring the use of lab equipment and causing significant time delays. For practical in-field biobattery usage, this usage of additional equipment and subsequent preparation time may be avoided by collection of bacteria specimen and media from the ambient environment. However, the availability of these resources would be highly dependent on the specific use environment and unavailability of exoelectrogenic bacteria and/or a liquid media would render the biobattery ineffective; this would especially be an issue in arid environments. A technique called lyophilization, or "freeze-drying," has also been used in previous studies as a potential method for mitigating this issue. Known exoelectrogenic, lab-cultured bacteria can be preloaded onto the battery's anode, freeze-dried for preservation, and then rehydrated at a later date to activate the biobattery. Although this method initially seems to alleviate the issue of on-site bacteria culturing, problems still exist with this method: i) the lyophilization process requires initial preparation with expensive, bulky lab equipment, which limits fabrication, ii) a nutrient-rich media to rehydrate and feed the bacteria must still be collected from the ambient environment, iii) the storage life of biobatteries with lyophilized bacterial cells is limited, and performance continuously degrades over several weeks [9].

This paper presents a paper-fabricated MFC that utilizes preloaded *Bacillus subtilis* endospores as an alternative to lyophilized bacterial cells. *B. subtilis* is a gram-positive, non-pathogenic self-mediated exoelectrogen capable of sporulation—a process by which vegetative cells generate robust, spherically shaped endospores with slowed metabolism [12,13]. These bacterial endospores developed as a survival mechanism, offering resistance to harmful or extreme conditions, such as heat, chemicals, desiccation, and starvation [12,14]. Only once favourable conditions are resumed, or once a select few specific germinant particles become detectable, will they enter germination, return to vegetative cells, and resume normal metabolism [12]. Endospores can persist for extended periods of time in this fortified, dormant state. Researchers at the University of Edinburgh and the Institute of Aerospace Medicine have teamed up to initiate a 500-year experiment to more closely control and observe the shelf-life of *B. subtilis* endospores, with the first 2 years of storage in extreme desiccated conditions resulting in no significant loss of bacteria viability [15]. There is even a reported case of 250-million-year-old endospores from a *Bacillus* species being uncovered within salt crystals and being successfully revived by researchers at West Chester University, achieving the status of the oldest microbe ever recovered [16]. Therefore, endospores may have the potential to extend the shelf-life of paper biobatteries if used in place of lyophilized bacterial catalysts.

In this paper, shelf-life analysis of preloaded B. subtilis endospores in uncontrolled, open-air lab conditions is shown over the course of 4 weeks, giving insight into the adequate storage conditions and respective stability of spores for applications in storable biobatteries. Furthermore, the presented paper MFC is designed specifically for activation with virtually any available fluid— specifically human bodily fluids—alleviating the requirement for activation by nutrient-rich environmental liquids and allowing for the biobattery to be effectively used in any situation. The biobattery contains a germinant layer above the endospore-residing anode layer, which stores all of the necessary nutrients and germinant materials for the endospores to germinate. Once bodily fluids are injected into the device inlet, these materials are washed into the anode to trigger germination and activate the MFC (Fig. 1a). A range of various fluids are evaluated and shown to effectively induce germination and result in bioelectric power generation, including artificial saliva, artificial sweat, artificial urine, and tap water. Specifically, artificial saliva was used to start up three biobatteries, which were then connected in series to achieve an open circuit voltage (OCV) of 0.56 V and a power output of 2.4 μW, successfully powering a digital thermometer.

2. Results and discussion

2.1. B. subtilis endospore germination on a paper substrate

Despite the fact that *B. subtilis* germination is not yet fully understood, there are particular conditions that tend to encourage endospores to germinate. Most effectively, *B. subtilis* spore germination can be triggered by the presence of several very specific nutrient germinants; the amino acids L-valine, L-alanine, and a combination of L-asparagine, glucose, fructose, and potassium chloride (AGFK) are amongst the most common germinants used in lab settings [12,13]. Involved in the detection and subsequent response to these nutrient germinants are highly specialized germination-dedicated membrane proteins, or germinant receptors (GRs) [13]. The three main GRs utilized by *B. subtilis* are GerA, GerB, and GerK; GerA is activated by L-valine and L-alanine while GerB and GerK are both simultaneously activated by AGFK [13]. Even after exposure to nutrient germinants and stimulation of the GRs, there often is a measurable time delay before a spore may commit to germination, ranging from several minutes to days [13]. This time delay is further lengthened—and percent germination rates reduced–when there are fewer GRs within the spore populations or when the nutrient germinant concentrations in the ambient environment are reduced [13]. There exist other methods of germination that may bypass the GR mechanism of endospores, achieving more rapid committal to germination with reduced time delays. One such method is spore exposure to very high pressure—on the scale of 500–1000 MPa—which ruptures the spores' coat, enabling instantaneous initiation of the germination, though practically achieving pressures of this degree pose an additional challenge [13,17]. This means of achieving rapid germination is not yet viable for use outside of controlled laboratory settings, and so it has not been evaluated in this study.

Our biobattery design utilizes preloaded bacterial endospores to be germinated within the vacancies of the paper fibers via the nutrient germinant-initiated germination pathways. To trigger germination, the endospores must effectively detect the applied nutrient germinants within the small pores of the paper substrate. The paper substrate used in this study (Whatman 3MM chromatography) has a pore size of approximately 6 μm, while *B. subtilis* spores are typically 1 μm in length and 0.5 μm in diameter and vegetative cells 1–6 μm in length and 1 μm in diameter [3,18,19]. Thus, once applied to the paper, the bacterial spore preparation can flow throughout the porous paper region while still being somewhat constricted by the pore size, which prevents all of the spores from sinking seeping through the entire thickness of the paper to accumulate on the bottom surface of the paper (Fig. S2a). This allows

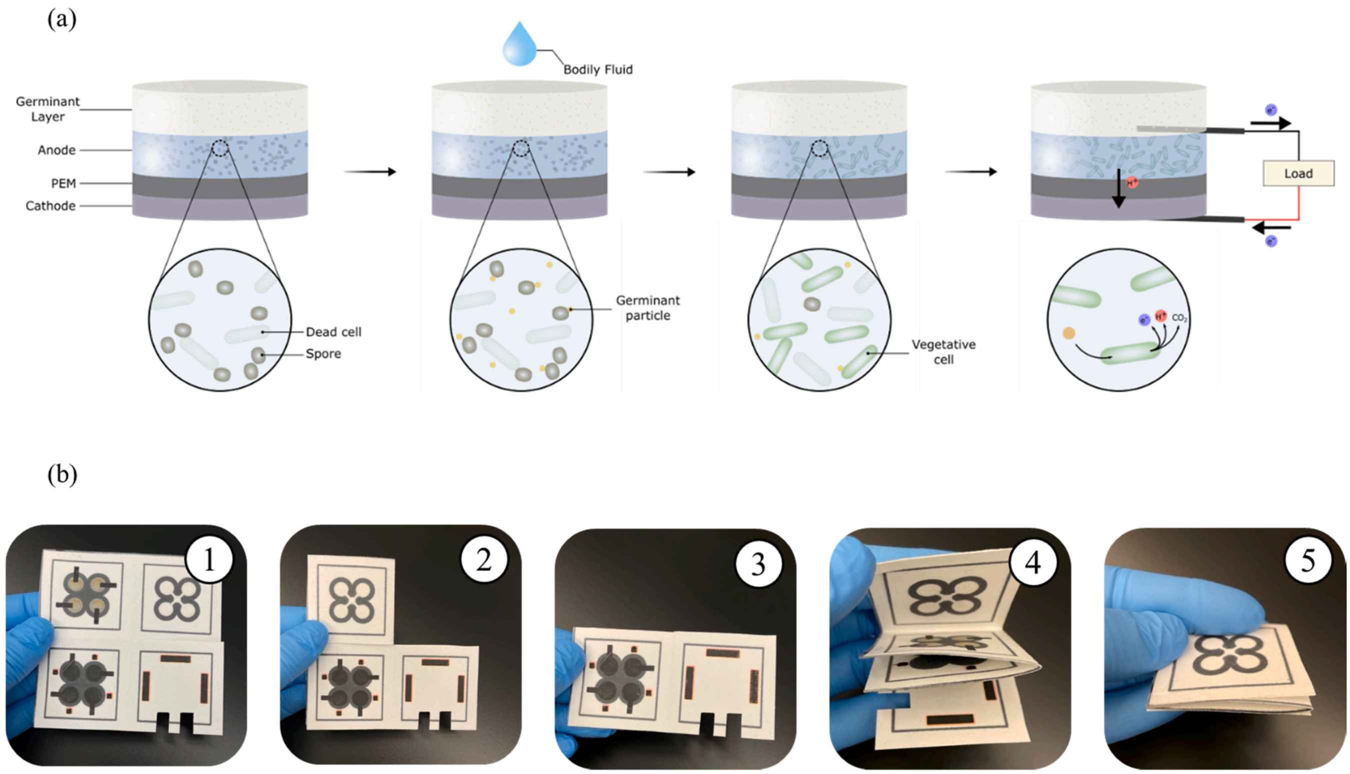

Fig. 1. (a) Conceptual image of bodily fluid activated microbial fuel cell based on the principle of bacterial endospore germination. (b) Photograph images of progressive folding steps for paper biobattery usage.

for a relatively even distribution of spores and firm attachment to the paper fibers, while maintaining sufficient space for nutrient exposure and cell outgrowth. To confirm both the germination capability within paper substrates and identify the baseline power generation parameters from the endospore-based biobatteries, experiments were first conducted on the paper biobattery without the use of a preloaded germinant layer. Instead, 30 µl of a liquid germinant mixture composed of L-valine, AGFK, and lysogeny broth (LB) was applied directly to each of the 4 MFC units' anode regions, containing the preloaded and air-dried bacterial spores. The resulting bioelectricity generation from a single MFC unit was monitored at specified intervals—0 h, 1 h, 2 h, and 3 h—aiding in determining the effects of gradual germination on the biobattery's output (Fig. 2a and b). The experiment was carried out on 10–12 identical MFCs, and the data was averaged for plot representation; error bars are additionally included for consistency evaluation. A consistent rise is observed in open circuit voltage (OCV), power density, and current density as the time delay, or germination time, is increased from 0 h to 3 h. The measurements taken at t = 0 h act as the experimental control group, as no spores have yet had the opportunity to germinate. Since t = 0 h data account for the inherent voltage differences between the cathode and the germinant solution and spore surfaces, the improvement in bioelectricity generation for successive measurements can be attributed entirely to germination progression. Once the spores have germinated and returned to a vegetative state, they resume normal respiratory cycles—the origin of the generated free electrons and bioelectricity generation. Therefore, as bioelectricity improves, we can assume more spores have reached this vegetative state (Fig. S1). The MFCs reached a maximum performance of 0.23 V OCV and 0.86 $\mu W/cm^2$ after 3 h of germination time, which can be assumed to be the time at which most of the spores have germinated. Beyond 3 h germination time produced no additional increase in voltage or power generation.

To verify the time durations required for *B. subtilis* germination, microscopic analysis was also performed. Endospores were loaded onto a paper substrate, saturated with the germinant mixture, and then harvested at the same specified time intervals used for bioelectricity measurement experiments: 0 h, 1 h, 2 h, and 3 h. The harvested cells were dyed with two fluorescence dyes: 5(6)-carboxyfluorescein diacetate (cFDA) and propidium iodide (PI). The cFDA causes vegetative bacterial cells to appear bright green, while PI stains both dead cells and bacterial spores, causing them to fluoresce a deep red. After staining, the bacterial cells are fixed to glass slides and observed under brightfield and fluorescence microscopy (Fig. 2c and Fig. S2b-c). In agreement with the growth trends seen from the bioelectricity experiments, the samples given more time immersed in the germinant solution-soaked paper displayed a larger percentage of vegetative, or green-dyed, cells in their corresponding microscopic images. The transition of the fluorescence microscopic images from red to green over the course of 3 h—with the t = 3 h interval image appearing almost entirely green with the exception of a few stray dead cells—confirms that the bacterial spores are capable of germinating on the paper substrate and that the time required for them to reach majority germination under these conditions is approximately 3 h.

2.2. Bodily fluid activation of microbial fuel cells

Previously, activation of MFCs and paper biobatteries have required the availability of environmental liquids rich in carbon sources, such as wastewater and concentrated biomass [20,21]. These liquids act as a nutritional source for bacterial respiration, supplying organic materials that can be broken down into glucose and subsequently used for energy, but liquid media with sufficiently high concentrations of organic material are not always available in the biobattery's intended use environment. Our biobattery was designed on the basis that the preloaded bacterial spores can be activated with a range of fluids, even the user's own human bodily fluids, relieving the battery's dependency on environmental conditions. Each MFC consists of a germinant paper layer stacked on top of the spore-containing anode layer. This germinant layer

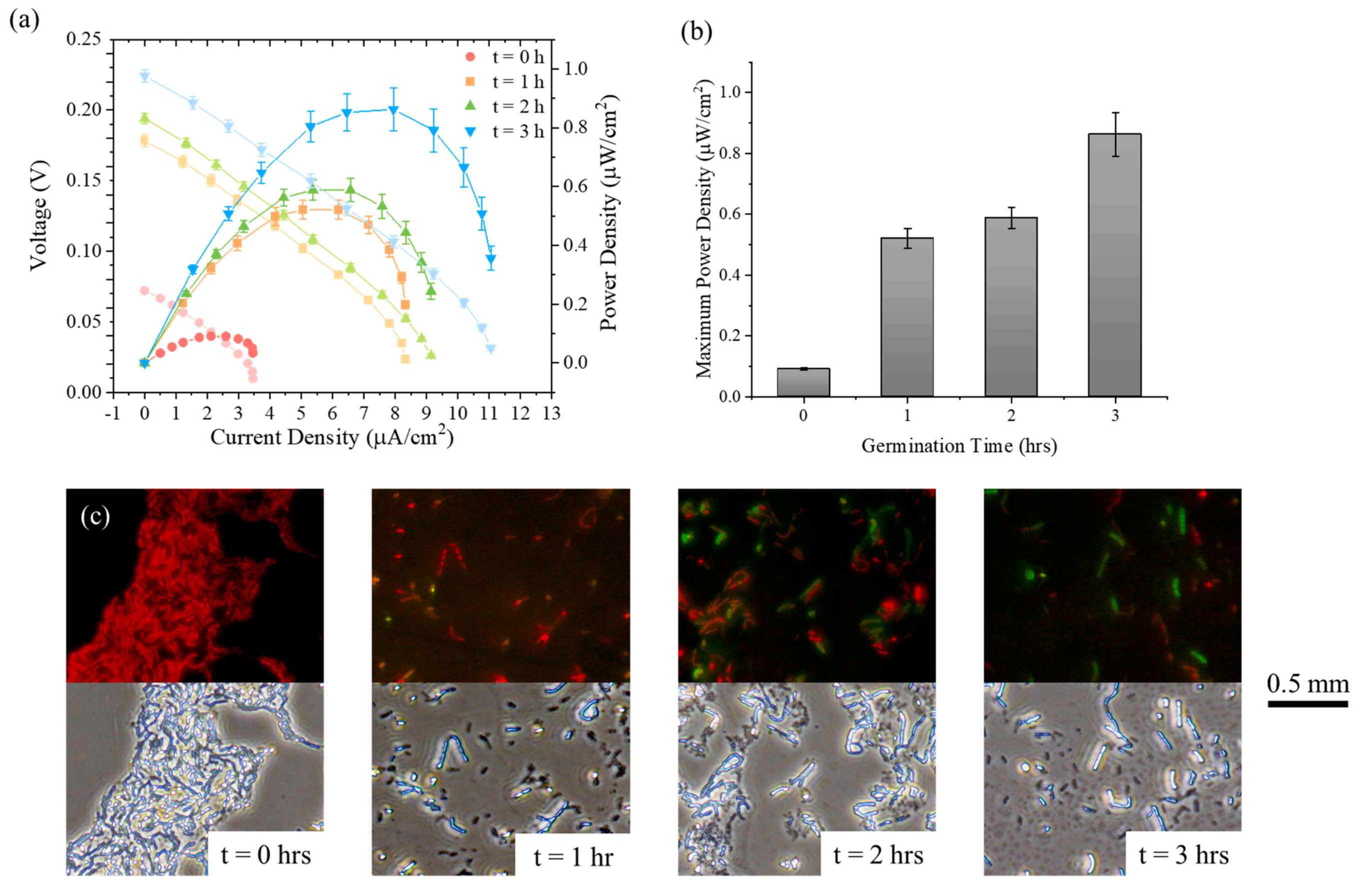

Fig. 2. (a) Polarization curve and power generation plot of individual paper MFCs when using liquid germinant mixture to activate the germination of preloaded *B. subtilis* endospores. (b) Comparison of biobattery's maximum power density as a function of allotted germination time. (c) Corresponding fluorescence and brightfield microscopic images of unpurified *B. subtilis* after 0 h, 1 h, 2 h, and 3 h allotted germination time on paper (60X mag).

is initially saturated with an L-valine, AGFK, and LB liquid mixture and dried. When the bodily fluids are introduced to the battery's germinant layer, these nutrient germinant particles and carbon-rich media remnants are carried into the anode region, exposing the spores to both the germinants required for germination initiation and the nutrients for maintaining their metabolism once they return to a vegetative status. Since there are reserves of germinants and carbon sources stored within the battery itself, the bodily fluids used to activate the battery may not be required to contain significant additional organic materials, allowing for biobattery to attain more flexibility of use.

The efficacy of the bodily fluid activated biobatteries was evaluated using four different fluids: artificial saliva, artificial sweat, artificial urine, and tap water. For each activation fluid, 100 μl of the fluid was introduced into the biobattery's inlet and bioelectricity generation of each individual MFC unit was measured after 0 h, 1 h, 2 h, and 3 h of germination time, as it was previously shown that it takes about 3 h for all of the endospores to germinate (Fig. 3). Each of these test cases were performed several times, about 10–12 cells for each fluid-time combination. Once again, there is a general trend of the OCV, power density, and current density increasing with longer germination times, implying the progressive germination of spores is achievable even in the cases in which the biobattery is activated with artificial bodily fluids or tap water. Ultimately, artificial saliva resulted in the highest output parameters, reaching an OCV of about 0.2 V, a power density of 0.44 μW/cm^2, and a current density of 7 μA/cm^2, even exceeding the bioelectricity output of similarly prepared and activated lyophilized-based MFCs (Fig. S5). In terms of maximum power density, artificial saliva was followed by sweat at 0.40 μW/cm^2, urine at 0.36 μW/cm^2, and then tap water at 0.32 μW/cm^2.

If neglecting the effects of inevitable inconsistencies in fabrication, the slight variation in maximum bioelectricity generation between biobatteries activated with different fluids likely stems from the fact that the pH, the conductivity, and the solutes added to each activation fluid vary in an attempt to mimic the characteristics of real bodily fluids (Table S2). This could unsymmetrically influence the measured bioelectricity generation in two ways: (1) the electrolytic characteristics of the solution could *directly* affect the electrical output, or (2) the components within the fluid and the resulting changes to environmental conditions may *indirectly* affect the bioelectrical output by influencing the growth of the bacterial population. In other words, higher conductivity and higher electrolytic strength within the fluid may positively influence the measured voltage potential across the battery as ions and electrons move through the fluid at larger volumes and faster speeds. On the other hand, specific components within the activation fluid as well as the resulting pH may simultaneously affect the speed of spore germination, metabolism, and population growth. The ideal activation fluid would be the optimal combination of these direct and indirect effects, which was found to be artificial saliva.

The ionic effect from the activation fluids, which is unrelated to our main focus of spore-derived bioelectricity, can be isolated and assessed through the t = 0 h data points in our presented plots. At t = 0 h, the spores were not given any time to achieve germination, and therefore are expected to be 100% spores, which should not actively contribute to the bioelectricity output. Therefore, the t = 0 h data primarily considers the electricity generated from the ions found within the activation fluid and from the materials stores within the germinant layer. However, the OCVs at t = 0 h are noted to be approximately 0.07 V for saliva, 0.06 V for sweat, and 0.04 V for urine and tap water, which is considerably

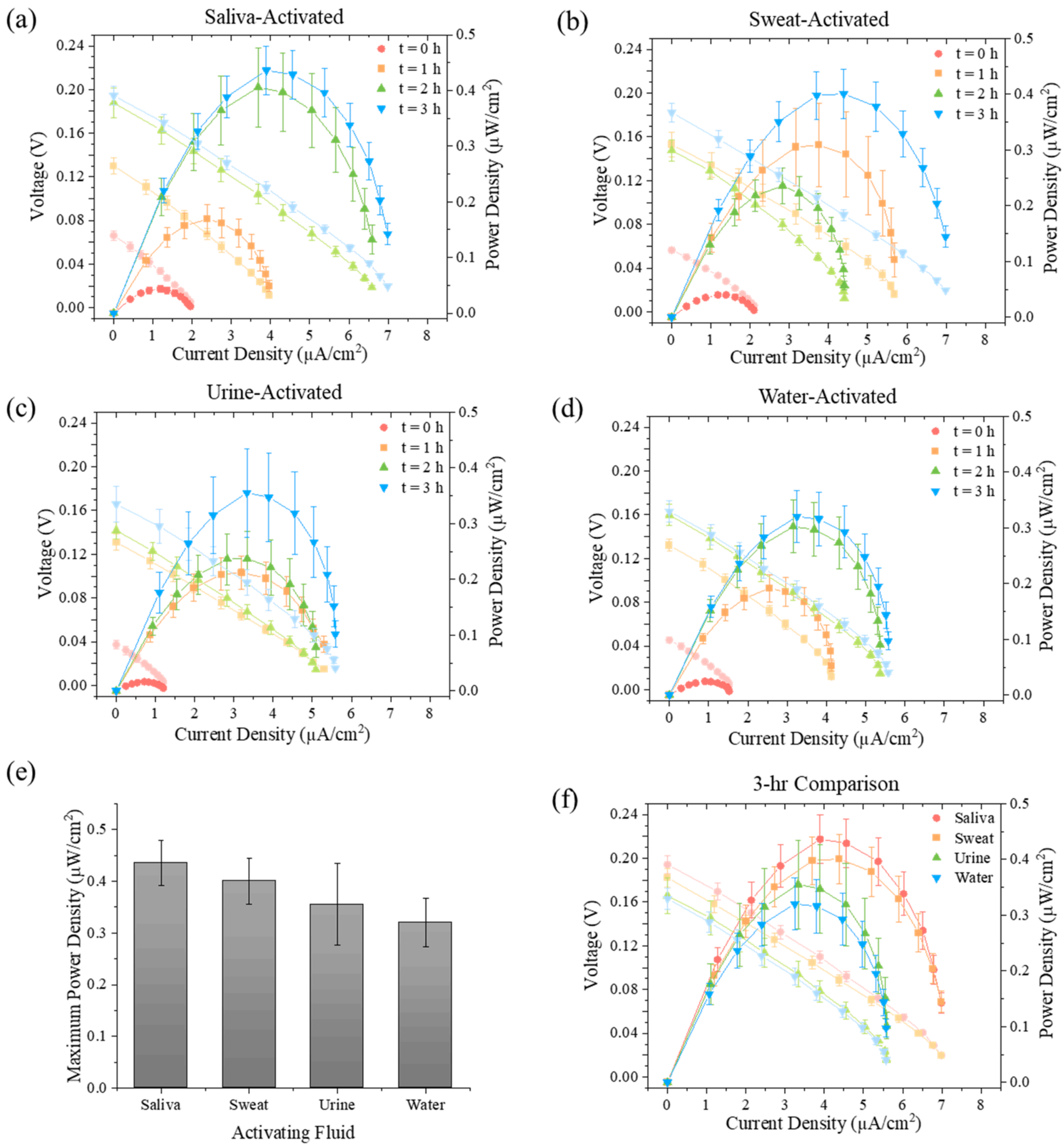

Fig. 3. Polarization curve and power density plot per MFC when activated with (a) artificial saliva, (b) artificial sweat, (c) artificial urine, and (d) tap water. (e) Comparison of attained power density of MFC for each activation fluid. (f) Superimposed comparison of polarization and power plots for each activation fluid at 3 h germination time.

lower than that of the maximum voltages attained after 3 h, indicating that bacterial metabolism rather than ions is the main source of electricity.

As for the effect of activation fluid constituents, with the exception of tap water, each artificial bodily fluid contains additional energy for the bacterial spores in the form of carbon-containing molecules, like glucose and L-lactate. Therefore, it would be expected that tap water would result in lower power generation as a result of reduced availability of nutrients for the cells' metabolism, which is indeed observed in the collected data. However, even with the absence of additional nutrient contents, activation with tap water still results in bacterial spore germination, as demonstrated by the progressive increase in power output over the course of 3 h germination time. This shows that the spore-based biobattery with a built-in germinant layer can be effectively activated by virtually any liquid, regardless of its nutrient contents; this includes both human bodily fluids, water, and other ambient environmental liquids.

2.3. Shelf-life analysis

One of the persisting issues surrounding the practical usage of paper-based biobatteries is their limited shelf-life capabilities. The shelf-life of biobatteries containing lyophilized bacterial cells has previously been investigated, revealing significant degradation in performance after a few weeks to months of storage [9]. After 16 weeks of storage time in ambient lab conditions, the lyophilized bacteria biobatteries experienced an estimated 35% decline in maximum power density, as extrapolated from published data [9]. In practice, it would likely take several weeks for biobatteries to be fully fabricated, prepared, distributed, and utilized by the consumer, necessitating storage stability on the scale of several months. As *B. subtilis* endospores embody a robust, highly protected bacterial state, spore-based biobatteries may further improve upon the stability displayed by lyophilized bacteria-based approaches. To confirm this assumption, bioelectricity output for our endospore-containing biobattery was monitored after increasingly long storage durations. The OCV, power density, and current density of individual MFC units were measured immediately after completed fabrication, and then after 1 week, 2 weeks, and 4 weeks of unoptimized, open-air storage within a lab setting. Each was activated with 30 µl per cell of the liquid germinant mixture. The fabricated biobatteries were stored unsealed, in ambient air to fully evaluate their shelf-life when stored in the lowest regulated conditions. The lab climate was maintained at about 22.8 °C and relative humidity ranged from about 30–50%.

As one may expect, there was still an observable reduction in bioelectricity generation for preloaded biobatteries that were stored for longer periods of time. MFCs used immediately following fabrication achieved an average of 0.86 µW/cm^2 and 0.23 V, while 1 week-stored MFCs achieved 0.66 µW/cm^2 and 0.22 V, 2 week-stored MFCs 0.56 µW/cm^2 and 0.20 V, and 4 week-stored MFCs 0.41 µW/cm^2 and 0.19 V (Fig. 4). This represents a 52% decrease in power density between the immediate-use case and the 4-week storage case. Though displaying a significant decrease in maximum power generation after 4 weeks of storage, the progressive reduction is likely caused by the unoptimized storage conditions negatively affecting the state of the endospores. Since the spores were dried onto the paper substrate and stored in open air, moisture from the air humidity could likely be easily absorbed by the paper fibers and the spores themselves. This moisture and oxygen exposure could contribute to more favorable environmental conditions, promoting a higher chance for random germination of some of the spores within the biobattery. The longer the storage time, the larger the percentage of these randomly germinated spores, and since these germinated cells cannot readily access sufficient nutrients, they likely quickly die after their germination. Altogether, this cycle of random

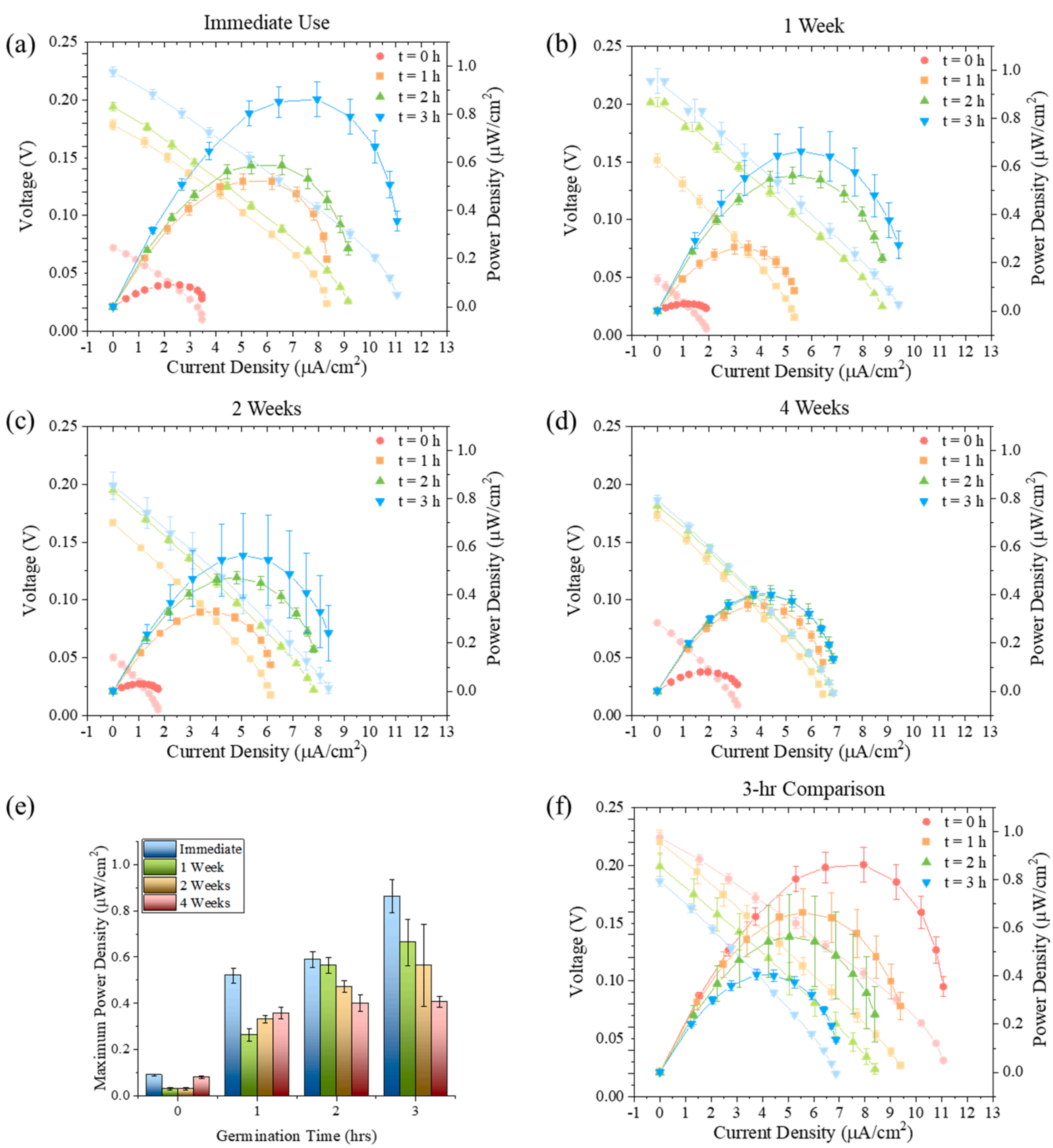

Fig. 4. Polarization curve and power density plot per MFC for biobatteries used (a) immediately after fabrication, (b) after 1 week of storage, (c) after 2 weeks of storage, and (d) after 4 weeks of storage. (e) Comparison of attained power density of MFC for each storage duration. (f) Superimposed comparison of polarization and power plots for each storage duration at 3 h germination time.

germination followed by rapid death lends to reduced spore viability over time when stored in humid open-air, causing the biobatteries to exhibit unoptimized shelf-life stability when left unsealed. However, according to first published data obtained from the 500 Year Microbiology Experiment, which is aimed at regularly evaluating the sustained viability of stored *B. subtilis* endospores over the course of a 500-year period, a sample of *B. subtilis* endospores has been shown to remain stable with no significant loss in viability for 2 years when kept in strictly desiccated, air-sealed containers [15]. So, although the paper biobatteries cannot practically be stored in the least-effort manner for extended periods of time, preserving the fully fabricated biobatteries within dry, air-tight seals may yet prove to significantly enhance the biobattery long-term stability.

2.4. Biobattery series connections and practical power generation

Bioelectricity output data has thus far been presented in the form of the average output of single MFC units, but each paper biobattery is composed of 4 individual MFCs with the capability of electrically connecting these 4 units in a series configuration. This allows for additive combination of the MFC voltages, enabling the biobatteries to supply power to applications with higher voltage requirements. The 4 MFCs within a biobattery are connected in series by simply folding over a quadrant of the paper pattered with graphite ink traces and through-hole vias. This serial connection mechanism was confirmed through comparison of the bioelectricity generation from an entire biobattery connected in series to the output of a single MFC unit (Fig. 5a). For this experiment, the biobatteries were activated with 100 μl artificial saliva and allotted 2 h germination time. Under these conditions, a single MFC generated approximately 0.21 V, 0.1 μW, and 1.7 μA, whereas the whole biobattery in a series configuration achieved 0.56 V, 2.4 μW, and 15.6 μA. The achieved voltage for 4 MFCs in series presents a voltage potential approximately 2.7 times that of a single cell. Though ideally 4 cells in series should be able to achieve 4 times that of a single cell to reach an OCV of 0.84 V, additional resistance from the graphite ink traces, variability in the individual MFCs, and shunt resistance from fluidic shorting in the germinant layer can likely account for this loss [22].

Although the 0.56 V and 2.4 μW of a single biobattery is likely sufficient for some integrated paper-based electronic systems, the practicability of our paper biobatteries was first demonstrated using digital thermometer due to its wide usage and availability. Basic digital thermometers, such as the one used here, conventionally use 1.5 V alkaline coin batteries. To ensure that the voltage ratings of the digital thermometer were met, 3 series-wiring. The 3 saliva-activated biobatteries were demonstrated to successfully power-up the thermometer and illuminate the electronic display (Fig. 5a).

3. Conclusion

In this work, we presented a biodegradable, paper biobattery activatable by virtually any available liquid, including bodily fluids which are the only 100% guaranteed activation fluid, as they can be non-invasively collected from the user. This allows for the biobattery to be practical in even the most remote and arid regions. Due to the incorporation of a germinant layer containing the necessary nutrient germinant particles and organic fuel, progressive germination and subsequent bioelectricity generation was exhibited from preloaded *B. subtilis* endospores after activation with artificial saliva, sweat, urine, and even tap water. Since each biobattery is composed of 4 individual MFCs, all of which can be serially connected through paper folding, the entire biobattery attained an OCV of 0.56 V. Additionally, with 3 of these serially connected biobatteries, it was possible to power a 1.5 V-rated digital thermometer. Though the performance of the biobatteries diminished after several weeks of storage in open-air, ambient lab conditions, the durable nature of endospores offers potential improvements to biobattery shelf-life if the storage conditions are optimized. Therefore, the paper biobatteries described in this paper present a step towards low-cost, practical, storable, paper-integrable energy sources for a range of paper-based electronic systems and low power sensors. The fact that they are unrestricted by nutrient-rich environmental liquid activation or locally derived exoelectrogenic bacteria enable power generation in nearly any location at any time.

4. Experimental procedure

4.1. Bacterial inoculum and sporulation

B. subtilis strain 168 was cultured from a bacterial stock by inoculating 20 ml of lysogeny broth (LB) and placing on a shaker at 50 rpm and 37 °C. The sporulation of *B. subtilis* was carried out through nutrient exhaustion on LB agar plates [10]. After being allowed to culture in the LB for 24–36 h, 200 μl of broth culture was transferred and spread onto an LB agar plate. To allow for nutrient exhaustion and majority sporulation of the bacteria, the culture was stored at 37 °C for an additional 3–5 d. The bacteria were then collected from the plate, suspended in distilled water, and pelleted by centrifugation at 4000 rpm for 4 min. This was repeated three times with intermediary rinsing with distilled water. The harvested spores were resuspended in distilled water and thermal treated at 80°C for 30 min to inactivate any remaining vegetative cells. The spores were tightly sealed in 15 ml centrifuge tubes and stored at 4°C.

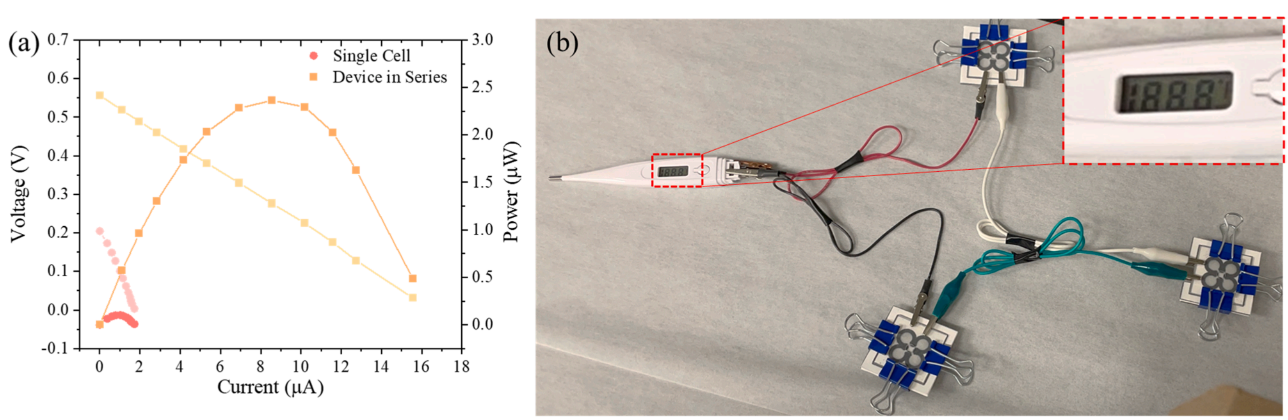

Fig. 5. (a) Polarization curve and power generation for an individual MFC unit vs. an entire biobattery connected in a series configuration, composed of 4 MFC units. (b) Demonstration of 3 serially connected, artifical saliva-activated biobatteries successfully powering a digital thermometer.

4.2. Bacterial endospore purification

Spore purification was carried out based on a modified version of Tavares' and Souza's second purification method [23]. The spores in distilled water were centrifuged for 10 min at 4000 rpm, and the supernatant was extracted from the tube using a micropipette. The spores were resuspended in a phosphate-buffered saline (PBS) containing 50 µg/ml lysozyme. After vortexing, the suspension was stored on a shaker for 1 h at 37 °C. The spores were rinsed with 1 vol of distilled water and resuspended in a 0.05% sodium dodecyl sulfate (SDS) solution. The cells were then rinsed 3 times with distilled water. The resulting spores from 8 agar plates were then combined, achieving approximately 1 ml of purified spores per tube. The spores were then either stored as a pellet or resuspended in 2 ml DIW for application on the device anode.

4.3. Germinant and artificial bodily fluid preparation

To prepare the germinant mixture, LB medium was mixed with L-Valine (10 mM) and AGFK (10 mM L-Asparagine, 33.6 mM D-Glucose, 33.6 mM D-Fructose, 60 mM KCl), all of which was obtained from Sigma-Aldrich. Artificial saliva (AFNOR NFS91–141) was purchased from Pickering Laboratories, artificial sweat (1190–01, Level 2) was purchased from Quantimetrix, and artificial urine (470024–546) was purchased from Ward's Science. The artificial bodily fluids were further modified with L-lactate and glucose to replicate the carbon source concentrations of the average human [9,24–27]; 0.1 mg/ml glucose and 0.0225 mg/ml L-lactate was added to the artificial saliva, 0.5 mg/ml glucose and 2 mg/ml L-lactate was added to the artificial sweat, and 0.15 mg/ml glucose was added to the artificial urine.

4.4. Bioelectricity measurement

With a sample rate of 1 S/s, the voltage difference between the anode and cathode battery electrodes was monitored using a Model DI-4108 High Speed DAQ acquired from DATAQ Instruments. Automatic polarization tests were run using the customized data acquisition system, measuring the potential across 14 decreasingly resistive loads: 470 kΩ, 240 kΩ, 160 kΩ, 100 kΩ, 75 kΩ, 47 kΩ, 33 kΩ, 22 kΩ, 15 kΩ, 10 kΩ, and 2 kΩ. Generated current and power data were calculated using the resistance values and the corresponding recorded voltage potential. By dividing current and power values by the MFC anodic area of 0.28 cm^2, current density and power density values were obtained.

4.5. Fluorescence dyeing and microscopy

To visualize germination progression, the germinant-exposed spores were double-stained with 5(6)-carboxyfluorescein diacetate (cFDA) and propidium iodide (PI), causing germinated cells to fluoresce bright green and endospores or dead cells to fluoresce red. The staining process was carried out before slide fixation to avoid washing mobile bacterial cells off the slide. The two dyes were prepared by dissolving 2 mg cFDA powder into 1 ml dimethyl sulfoxide (DMSO) and 1 mg PI into 1 ml distilled water. For each sample, 1 ml of bacterial cells at an optical density of 0.75 OD_{600} was used. The cell suspension was centrifuged for 4 min at 4000 rpm, the supernatant was removed, and the cells were resuspended in 2 ml PBS with 2.5 µl cFDA. After incubation for 5 min at 37 °C, the sample was once again centrifuged, the supernatant removed, and suspended in 2 ml of PBS and 13 µl PI. The sample was mixed, centrifuged, and rinsed with 1 vol of distilled water before being resuspended in 1 ml of distilled water. Cells were fixed to glass slides and viewed with brightfield and fluorescence microscopy (Nikon Eclipse TS100).

4.6. Fabrication and storage of biobattery

Each biobattery contains 4 MFCs and each of these MFCs is composed of four basic paper layers: a germinant layer containing the preloaded and dried germinant mixture, a conductive anodic layer with preloaded endospores, a layer containing both the wax-based proton-exchange membrane (PEM) and the cathodic catalyst region, and a layer with conductive traces that allow for all 4 MFCs to be electrically connected in series (Fig. S3 & S4).

The entire device is fabricated on a Whatman 3MM chromatography paper substrate. The chromatography paper was printed (ColorQube 8570) with a wax-based ink and baked at 140 °C for 1 min to create penetrative hydrophobic barriers throughout the paper fibers. A thin layer of wax ink was additionally pattered on one side of the cathodic paper layer to act as the ion-exchange membrane, or the ionic separator between the anode and cathode regions.

First, the germinant paper layer was prepared by applying 120 µl of the germinant mixture to the wax-enclosed germinant region. The paper was air-dried for several hours within a laminar flow hood to limit contamination of the nutrient-rich media.

To functionalize the anodic paper region, a conductive, hydrophilic, bio-compatible ink was concocted by mixing 2 ml of 1 wt% poly(3,4-ethylenedioxythiophene): polystyrene sulfonate (PEDOT: PSS) and 100 µl dimethyl sulfoxide (DMSO). When applied to the paper substrate, this mixture enables the paper fibers to act as a hydrophilic, conductive network. Since the germinated bacteria will remain in close, direct contact with these paper fibers, this allows for more rapid collection and transfer of the free electrons to the nearby electrode [28]. This anodic ink was thoroughly mixed through sonication for 90 min at 69°C. Immediately following sonication 10 µl of ink was applied to each MFC's paper anode using a micropipette and allowed to air dry for several hours. Once dried, 30 µl of the harvested and purified endospores were loaded onto the anode and air-dried.

The cathodic catalyst used within the cathodic paper region was made by mixing 2 ml PEDOT: PSS, 100 µl DMSO, and 100 mg silver (I) oxide (Ag_2O). Similar to the anodic ink process, this Ag_2O-based ink was sonicated for 90 min at 69°C, and then 8 µl was micropipetted onto each paper cathode region.

The anodic electrode, cathodic electrode, and serial connection traces were all applied to the paper biobattery through screen-printing of a conductive graphite ink (E3449, Ercon Inc., USA).

CRediT authorship contribution statement

Mya Landers: Investigation; Methodology; Data curation; Writing – original draft. **Seokheun Choi**: Conceptualization; Supervision; Project administration; Funding acquisition; Writing – review, editing, and finalization.

Declaration of Competing Interest

The authors declare that they have no known competing financial interests or personal relationships that could have appeared to influence the work reported in this paper.

Acknowledgments

This work was supported mainly by the National Science Foundation (CBET #2100757, ECCS #2020486, and ECCS #1920979), and partially by the Office of Naval Research (#N00014-21-1-2412).

Appendix A. Supporting information

Supplementary data associated with this article can be found in the online version at doi:10.1016/j.nanoen.2022.107227.

References

[1] C. Dincer, R. Brich, E. Costa-Rama, M.T. Fernandez-Abedul, A. Merkoci, A. Manz, G.A. Urban, F. Guder, Disposable sensors in diagnostics, food, and environmental monitoring, Adv. Mater. 31 (2019), 1806739, https://doi.org/10.1002/adma.201806739.

[2] J.R. Mejia-Salazar, K.R. Cruz, E.M.M. Vasques, O. Novais de Oliveira Jr., Microfluidic point-of-care devices: new trends and future prospects for eHealth diagnostics, Sensors 20 (2020) 1951, https://doi.org/10.3390/s20071951.

[3] E. Evans, E.F.M. Gabriel, W.K.T. Coltro, C.D. Garcia, Rational selection of substrates to improve color intensity and uniformity on microfluidic paper-based analytical devices, Analyst 139 (2014) 2127–2132, https://doi.org/10.1039/C4AN00230J.

[4] H. Shamkhalichenar, C.J. Bueche, J.-W. Choi, Printed circuit board (PCB) technology for electrochemical sensors and sensing platforms, Biosensors 10 (2020) 159, https://doi.org/10.3390/bios10110159.

[5] S. Kuchhal P, Battery waste management, in: Environmental Science and Engineering, Vol. 5, Solid Waste Management Stadium Press LLC, USA, 2017, pp. 141–155.

[6] A. Fraiwan, S. Mukherjee, S. Sundermier, H.-S. Lee, S. Choi, A paper-based microbial fuel cell: instant battery for disposable diagnostic devices, Biosens. Bioelectron. 49 (2013) 410–414, https://doi.org/10.1016/j.bios.2013.06.001.

[7] Y. Gao, S. Choi, Stepping toward self-powered papertronics: integrating biobatteries into a single sheet of paper, Adv. Mater. Technol. 2 (2017), 1600194, https://doi.org/10.1002/admt.201600194.

[8] L. Liu, S. Choi, Enhanced biophotoelectricity generation in cyanobacterial biophotovoltaics with intracellularly biosynthesized gold nanoparticles, J. Power Sources 506 (2021), 230251, https://doi.org/10.1016/j.jpowsour.2021.230251.

[9] M. Mohammadifar, S. Choi, A papertronic, on-demand and disposable biobattery: saliva-activated electricity generation from lyophillized exoelectrogens preinoculated on paper, Adv. Mater. Technol. 2 (2017), 1700127, https://doi.org/10.1002/admt.201700127.

[10] J. Ryu, S. Choi, Bioelectricity production from sweat-activated germination of bacterial endospores, Biosens. Bioelectron. 186 (2021), 113293, https://doi.org/10.1016/j.bios.2021.113293.

[11] M. Tahernia, E. Plotkin-Kaye, M. Mohammadifar, Y. Gao, M.R. Oefelein, L.C. Cook, S. Choi, Characterization of electrogenic gut bacteria, ACS Omega 5 (2020) 29439–29446, https://doi.org/10.1021/acsomega.0c04362.

[12] P.T. McKenney, A. Driks, P. Eichenberger, The Bacillus subtilis endospore: assembly and functions of the multilayerer coat, Nat. Rev. Microbiol. 11 (2013) 33–44, https://doi.org/10.1038/nrmicro2921.

[13] P. Setlow, Germination of spores of Bacillus species: what we know and do not know, J. Bacteriol. 196 (2014) 1297–1305, https://doi.org/10.1128/JB.01455-13.

[14] W.L. Nicholson, N. Munakata, G. Horneck, H.J. Melosh, P. Setlow, Resistance of Bacillus endospores to extreme terrestrial and extraterrestrial environments, Microbiol Mol. Biol. Rev. 64 (2000) 548–572, https://doi.org/10.1128/MMBR.64.3.548-572.2000.

[15] N. Ulrich, K. Nagler, M. Laue, C.S. Cockell, P. Setlow, R. Moeller, Experimental studies addressing the longevity of Bacillus subtilis spores - The first data from a 500-year experiment, PLoS One 13 (2018), e0208425, https://doi.org/10.1371/journal.pone.0208425.

[16] R.H. Vreeland, W.D. Rosenzweig, D.W. Powers, Isolation of a 250 million-year-old halotolerant bacterium from a primary salt crystal, Nature 407 (2000) 897–900, https://doi.org/10.1038/35038060.

[17] K. Reineke, A. Mathys, V. Heinz, D. Knorr, Mechanisms of endospore inactivation under high pressure, Trends Microbiol 21 (2013) 296–304, https://doi.org/10.1016/j.tim.2013.03.001.

[18] M. Carrera, R.O. Zandomeni, J. Fitzgibbon, J.-L. Sagripanti, Difference between spore sizes of Bacillus anthracis and other Bacillus species, J. Appl. Microbiol 102 (2006) 303–312, https://doi.org/10.1111/j.1365-2672.2006.03111.x.

[19] J. Errington, L.T.V. Aart, Microbe profile: Bacillus subtilis: model organisms for cellular development, and industrial workhorse, Microbiology 166 (2020) 425–427, https://doi.org/10.1099/mic.0.000922.

[20] H. Liu, R. Ramnarayanan, B.E. Logan, Production of electricity during wastewater treatment using a single chamber microbial fuel cell, Environ. Sci. Technol. 38 (2004) 2281–2285, https://doi.org/10.1021/es034923g.

[21] A. Kumlanghan, J. Liu, P. Thavarungkul, P. Kanatharana, B. Mattiasson, Microbial fuel cell-based biosensor for fast analysis of biodegradable organic matter, Biosens. Bioelectron. 22 (2007) 2939–2944, https://doi.org/10.1016/j.bios.2006.12.014.

[22] I. Ieropoulos, J. Greenman, C. Melhuish, Microbial fuel cells based on carbon veil electrodes: Stack configuration and scalability, Int. J. Energy Res. 32 (2008) 1228–1240, https://doi.org/10.1002/er.1419.

[23] M.B. Tavares, R.D. Souza, W.B. Luiz, R.C.M. Cavalcante, C. Casaroli, E.G. Martins, R.C.C. Ferreira, L.C.S. Ferreira, Bacillus subtilis endospores at high purity and recovery yields: optimization of growth conditions and purification method, Curr. Microbiol. 66 (2013) 279–285, https://doi.org/10.1007/s00284-012-0269-2.

[24] S. Robinson, N. Dhanlaksmi, Photonic crystal based biosensor for the detection of glucose concentration in urine, Photon. Sens 7 (2017) 11–19, https://doi.org/10.1007/s13320-016-0347-3.

[25] M. Patterson, S.D.R. Galloway, M.A. Nimmo, Variations in regional sweat composition in normal human males, Exp. Physiol. 85 (2000) 869–875, https://doi.org/10.1111/j.1469-445X.2000.02058.x.

[26] C. Schabmueller, D. Loppow, G. Piechotta, B. Schutze, J. Albers, R. Hintsche, Micromachined sensor for lactate monitoring in saliva, Biosens. Bioelectron. 21 (2006) 1770–1776, https://doi.org/10.1016/j.bios.2005.09.015.

[27] S. Emaminejad, W. Gao, E. Wu, Z.A. Davies, H. Yin Yin Nyein, S. Challa, S.P. Ryan, H.M. Fahad, K. Chen, Z. Shahpar, S. Talebi, C. Milla, A. Javey, R.W. Davis, Autonomous sweat extraction and analysis applied to cystic fibrosis and glucose monitoring using a fully integrated wearable platform, PNAS 114 (2017) 4625–4630, https://doi.org/10.1073/pnas.1701740114.

[28] M. Tahernia, M. Mohammadifar, Y. Gao, W. Panmanee, D.J. Hassett, S. Choi, A 96-well high-throughput, rapid-screening platform of extracellular transfer in microbial fuel cells, Biosens. Bioelectron. 162 (2020), 112259, https://doi.org/10.1016/j.bios.2020.112259.

Mya Landers is currently an electrical engineering M.S. student under the supervision of Dr. Seokheun Choi at SUNY Binghamton. She also received her B.S. from SUNY Binghamton in 2021. Her current research focuses on paper-based power solutions and paper electronics.

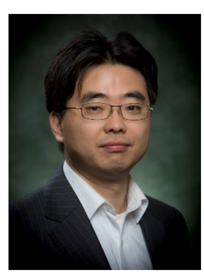

Seokheun Choi received his B.Sc. and M.Sc. degrees in electrical engineering from Sungkyunkwan University, Korea, in 2003 and 2004, respectively. He received his Ph.D. degree in electrical engineering from Arizona State University, USA, in 2011. He was a research engineer with LG Chem, Ltd., Korea, from 2004 to 2006. From 2011–2012, he was a research professor at the University of Cincinnati, USA. He is currently a Professor in the Department of Electrical & Computer Engineering at SUNY-Binghamton. Also, he is serving as a Director of the Center for Research in Advanced Sensing Technologies and Environmental Sustainability at SUNY-Binghamton.